REMOTE SENSING OF OPTICALLY SHALLOW, VERTICALLY INHOMOGENEOUS WATERS: A MATHEMATICAL MODEL *

W. D. Philpot and S. G. Ackleson
College of Marine Studies
University of Delaware

SUMMARY

A multiple-layer radiative transfer model of a vertically inhomogeneous, optically shallow water mass is briefly described. This model is directed toward use in remote sensing of water properties. Some preliminary results and qualitative predictions are presented.

INTRODUCTION

In most applications of remote sensing involving water quality the assumption is made that the water is vertically homogeneous. Usually the water is also assumed to be optically deep, i.e. absorption and reflection by the bottom are taken to be negligible. These assumptions are frequently adequate, as evidenced by the wide-ranging success in using remote sensing for observation of water properties. However, some concern has been voiced with respect to the general validity of the standard assumptions (ref. 1) and, in at least one case, a changing vertical distribution of material in water has been linked to variation in remote observations (ref. 2). It is the underlying thesis of the work presented here that vertically inhomogeneous and/or optically shallow waters are fairly common, that the inhomogeneity will affect the remotely sensed upwelling radiance and, therefore, that there is need for a mathematical model applicable to these situations and useful for remote sensing applications.

In the following pages a multiple-layer radiative transfer model of an optically shallow water mass is briefly described. In order for this model to be directly useful in remote sensing applications it must be invertible. This requirement necessitates several simplifying assumptions which will inevitably limit the accuracy of the model in at least some situations. Hopefully the advantages to be gained by having an easily manipulated model of a rather complex system should outweigh the loss in accuracy. Initially it is intended only that the model give a good qualitative description of the system, although care has been taken to formulate the model in such a way as to facilitate using the model to make quantitative predictions.

*This work was supported in part by Sea Grant contract # NA 80 AA-D-00106.

DESCRIPTION OF THE MODEL

Assumptions and Definitions

Radiative transfer models tend to be extraordinarily complex and utterly resistant to inversion. Much of the complexity arises because of the difficulty in describing anisotropic light fields. While the anisotropy is an important part of the interaction of light with water, it need not be described in minute detail. Characterization of the light field in general terms should provide the simplification necessary for deriving a model capable of describing a vertically inhomogeneous system but still susceptible to inversion.

The basic assumption is that the underwater light field may be effectively characterized by the apparent optical properties: the diffuse attenuation coefficients for upwelling and downwelling irradiance, the irradiance reflectance, and the radiance reflectance. The diffuse attenuation coefficient for downwelling irradiance is defined as

$$k_d(z) = \frac{-1}{E_d(z)} \frac{dE_d(z)}{dz} \tag{1}$$

where $E_d(z)$ is the downwelling irradiance at depth z. Likewise, the diffuse attenuation coefficient for upwelling irradiance is defined as

$$k_u(z) = \frac{-1}{E_d(z)} \frac{E_u(z)}{dz} \tag{2}$$

The diffuse attenuation coefficient will be dependent to some extent on the radiance distribution. However, evidence is growing that the underwater radiance distribution does not vary in a way that strongly affects the diffuse attenuation. In fact, observations by Baker and Smith (ref. 3) indicate that the diffuse attenuation coefficient for downwelling irradiance is remarkably insensitive to the radiance distribution, whether due to changes in sun angle or depth.

The irradiance reflectance, R(z), is defined as

$$R(z) = \frac{E_u(z)}{E_d(z)} \tag{3}$$

The term R(z), which has become a fairly standard measure of water color, is seemingly independent of illumination conditions (refs. 4 and 5). We may also define a radiance reflectance:

$$R_L(z,\theta) = \frac{L_u(z,\theta')}{E_d(z)} \tag{4}$$

where $L_u(z,\theta')$ is the upwelling radiance at depth z and in direction θ'.

In addition to the above standard properties we define two other parameters: the irradiance scattering function for downwelling light, $B_d(z)$, and a single-scattering irradiance attenuation coefficient for upwelling light, $k'(z)$. $B_d(z)$ is defined as the irradiance $dE_w(z)$ scattered upward at depth z from a horizontal slab of thickness dz when illuminated by the downwelling irradiance, $E_d(z)$:

$$B_d(z) = \frac{dE_w(z)}{E_d(z)dz} \tag{5}$$

The scattered irradiance, $E_w(z)$, is attenuated as it proceeds toward the water surface. However, the irradiance attenuation coefficient for upwelling light, $k_u(z)$, is not appropriate since it implicitly includes the backscattering of downwelling light already described by $B_d(z)$. To adjust for this we define a single-scattering irradiance attenuation coefficient, $k'(z)$, such that:

$$k'(z) = k_u(z) - B_d(z) \tag{6}$$

Like the other apparent properties, $B_d(z)$ and $k'(z)$ will be assumed to be quasi-inherent optical properties since they are dependent on the radiance distribution in essentially the same way as k_d, R_L, and R.

Model Geometry and Final Equations

This model treats the water as a plane-parallel medium of arbitrary depth in which the optical properties, depth and thickness of each layer, as well as the depth of the water and the bottom reflectance, may be specified independently. Figure 1 illustrates the model geometry for the relatively simple situation of one layer of turbid water in an otherwise homogeneous water column. The attenuation coefficients of pure water are k_w and k'_w, while the irradiance scattering function for pure water is B'_w. The corresponding optical properties of homogeneously distributed substances in the water are $n_s k_s$, $n_s k'_s$ and $n_s B'_s$ where n_s is a concentration parameter which may vary

between 0 and 1. For $n_s = 0$ the concentration of the material is zero. For $n_s = 1$ the concentration of the material is a maximum, i.e., the water has been replaced entirely by the substance.

An intermediate layer is shown in figure 1. This layer contains material which is optically distinct from the surrounding water. The optical properties of the material present in the layer are $n_\ell k_\ell$, $n_\ell k'_\ell$ and $n_\ell B'_\ell$, in complete analogy to the homogeneously distributed material.

A portion of the irradiance above the water surface, E_o, is reflected at the air water interface, $(S_a E_d)$. The remainder is transmitted $([1-S_a]E_d)$. The irradiance is attenuated as it passes down through the water column. At depth z, a portion of the downwelling irradiance is scattered back toward the water surface. This scattered irradiance is further attenuated as it travels to the surface and across the air-water interface.

A portion of the downwelling irradiance reaches the bottom (z = d) and is diffusely reflected there (A_d). The reflected portion is attenuated as it travels upward through the water column. The irradiance is affected by the local optical properties at each depth which are assumed to be constant within each layer.

The irradiance reflectance immediately below the water surface is given by

$$R(0-) = \frac{B_o}{k_o} \sum_{j=0}^{m} e^{-\sum_{i=0}^{j}(K_i-K_o)\Delta z_i} \left[e^{-K_o(h_j+\Delta z_j)} - e^{-K_o h_{j+1}} \right]$$

$$+ \sum_{j=1}^{m} \frac{B_i}{K_j} e^{-\sum_{i=0}^{j-1}(K_i-K_o)\Delta z_i} e^{-K_o h_i} \left[1-e^{-K_j \Delta z_j} \right] \qquad (7)$$

$$+ A_d e^{-K_o d} e^{-\sum_{i=0}^{m}(K_i-K_o)\Delta z_i}$$

where: $k_o = (1-n_s)(k_w + k'_w) + n_s\ (k_s + k'_s)$

$B_o = (1-n_s)B_w + n_s\ B_s \quad = B_d(z)$ for homogeneous regions

m = number of intermediate layers

h_i = depth to the top of layer i

Δz_i = thickness of layer i

$K_j = (1-n_s-n_i)\ (k_w+k'_w) + n_s\ (k_s+k'_s) + n_i\ (k_i+k'_i)$

$B_j = B_d(z) \quad$ for $h_i<z<h_i+\Delta z$

k_i = downwelling irradiance attenuation coefficient for layer i

k'_i = upwelling irradiance attenuation coefficient for layer i

n_i = concentration parameter for layer i

and where $\Delta z_o = h_o = 0$ and $h_{m+1} = d$. The first term on the right hand side of equation (7) describes the portion of $R_L(\theta')$ due to scattering from all the areas in which only the homogeneously distributed material is present; the second term describes the return from each of the layers; the third term accounts for the bottom reflectance. In deriving equation (7) it was assumed that none of the layers overlapped.

The irradiance reflectance is related to the observations immediately above the water surface by:

$$R = \frac{L_u(\theta) - \rho_a(\theta)\ L_k(\theta)}{(1 - S_a)E_d + E_r} \cdot \frac{Q(\theta')\ n_w^2}{1-\rho_w(\theta')} \qquad (8)$$

where: $L_u(\theta)$ = upwelling radiance above the water surface in direction θ

$L_k(\theta)$ = downwelling sky irradiance in direction θ

$\rho_a(\theta)$ = specular reflection at the water surface in air

$\rho_w(\theta')$ = specular reflection at the water surface

S_a = diffuse reflectance of the air-water surface

n_w = index of refraction of water

E_d = downwelling irradiance above the water surface

E_r = portion of the upwelling irradiance internally reflected in the water

$Q(\theta')$ = conversion factor relating radiance and irradiance reflectance

The above equations were derived in analogy to single-scattering radiative transfer models and as such will be called a single-scattering irradiance model (SSI). The primary distinction between the (SSI) model and two flow theory is that the downward scattering of upwelling light is ignored. This simplification causes results for strongly scattering waters to be inaccurate. In spite of its appearance, equation (7) is a relatively crude representation of the reflectance characteristics of an optically shallow, vertically inhomogeneous water body. The simplifying assumptions used in deriving equation (7) will limit the absolute accuracy of the model; however, it should provide a good qualitative description of variations in ocean color. Moreover, this model may be accurate enough in some situations to yield moderately accurate quantitative predictions.

APPLICATION OF THE RADIANCE MODEL TO AN OPTICALLY SHALLOW, HOMOGENEOUSLY ABSORBING WATER COLUMN

Upon formulation of the radiative transfer model for the case of an optically shallow, homogeneously absorbing water column, measurements of volume reflectance were conducted under the controlled conditions of a water tank. In an attempt to maintain a simple and inexpensive experimental design, sunlight was utilized as the illumination source. Variations in the absorptive capacity of the water as well as in column depth were considered.

Model Formulation

In applying the radiance model to the case of an optically shallow, homogeneously absorbing water column, a number of simplifications may be applied to equation (7). Each simplification is based upon one or more of the following assumptions:

1) the water column contains no intermediate layers possessing unique optical properties ($\Delta z = 0$)

2) the concentration of any particulate scattering material suspended throughout the water column is very small

3) the bottom is highly reflective and closely resembles a completely diffuse reflector

4) internally reflected irradiance, E_r, is negligible

5) observations are made in the nadir direction $\theta = 0$

Combining equations (7) and (8) and applying the above assumptions results in the relationship

$$\frac{L_u}{E_d} = \frac{(1-\rho_w)\ (1-S_a)}{Q\ n_w^2}\ A_d e^{-k_1 d} + \rho_k L_k \qquad (9)$$

Experimental Apparatus

Experiments were conducted using the cubic meter tank illustrated in figure 2. The sides of the tank were painted with a low-reflectance, ultra-flat black paint; the floor of the tank was coated with a high reflectance, flat white paint in order to optimize the return signal. Shadows from the sides of the tank were avoided by conducting all the measurements at a time when the sun was highest. At no time was the solar zenith angle greater than 35^o.

Radiance measurements were made using a United Detector Technology Spectral Radiometer designed to continuously scan the visible and near infrared portion of the light spectrum from 400nm to 1100nm. As shown in figure 2, the radiometer was positioned directly over the center of the tank so as to record upwelling radiance in the zenith direction. In this configuration the radiometer shaded the water surface directly underneath from downwelling sky radiance. Therefore, the reflectance term ($\rho_k L_k$) on the right side of equation (9) may be neglected.

The total downwelling solar irradiance was measured with the use of a panel coated with a standard reflectance medium, barium sulphate. Such a coating is noted for its high reflectance and close resemblance to a Lambertian reflector.

Experimental Procedure

Prior to filling the tank with any water the bottom albedo, A_d, was measured directly. The wavelength range considered for this measurement, as well as all others to be presented, was from 400nm to 700nm in increments of 20nm. After measuring A_d, several water types varying in absorptive capacity were added to the tank one at a time. The absorptance of each water type was controlled by adding known quantities of rhodamine dye.

Table 1 is a summary of the physical characteristics associated with each water type considered. In each case, volume reflectance was calculated by normalizing the recorded upwelling radiance from the tank to that reflected from the barium sulphate panel. Thus,

$$R = \frac{L_u}{E_d} = \frac{0.79\ L_u}{\pi L_{RP}} \qquad (10)$$

where 0.79 is the reflectance of the barium sulphate panel.

The only variable within equation (9) not directly measured was K_1. Values were calculated by simultaneously solving equation (9) for two different depths of each water type which yields

$$K_1 = \frac{\ln(R_1/R_2)}{d_2 - d_1} \tag{11}$$

Values chosen for the constant terms in equation (9) are as follows: $S_a = 0.06$, $\rho_w = 0.02$, $Q = \pi$, and $n_w = 1.33\text{-}1.39$. The latter range of values reflects the dependence of n_w upon the wavelength considered.

Results and Conclusions

Figure 3 is a plot of K_1 versus wavelength for each of the water types considered. With the addition of 2.7 ppm rhodamine dye to the tap water the value of K_1 increase sharply in the high absorption region between 480nm and 580nm. A maximum value occurs at 560nm. From 580nm to 700nm, K_1 drops to near that of clear tap water. The same trend, only more exaggerated, occurs for tap water with the addition of 10.8ppm rhodamine dye; the width of the absorption band increases to include 460nm and 580nm, and the absorption peak occurs at 540nm rather than 560nm.

In each water type with dye added, similar values of K_1 occur between 600nm and 700nm. It is interesting to note that such values are lower than those representing clear tap water with no dye added. Clearly, the dye is transparent for longer wavelengths which accounts for its characteristic red tinge. Yet, intuitively, this window should not be any more transparent than the clear water to which the dye was added. If indeed equation (10) accurately describes K_1, then the differing values in the longer wavelengths could be a result of the varying quality of the tap water used in the preparation of each water type. It was noted in the case of the clear tap water that the water used appeared to have a slight green tinge about it. As such, an associated absorption band in the red portion of the spectrum could account for the shape of the clear water curve. The tinge was not noticed in preparing either of the solutions containing rhodamine dye.

According to equation (11), the total attenuation coefficient may be calculated in terms of the change in upwelling radiance with respect to the change in water depth. The calculated values of K_1 are thus independent of bottom albedo. Rewriting equation (9) in terms of the bottom albedo with $Q = \pi$ and ignoring the reflectance term yields the relationship

$$A_d = \frac{\pi L_u n_w^2}{E_d(1-S_a)(1-\rho_w)} e^{K_1 d} \tag{12}$$

Utilizing equation (12), model predictions for A_d were derived in terms of the calculated values of K_1. As a comparison to the direct measurements of A_d, the calculated values of A_d as well as those directly measured were plotted with respect to wavelength and are presented in figure 4.

Model predictions for A_d were found to be quite similar to the directly measured values. A statistical correlation coefficient, r, was calculated as a measure of the similarity between the two curves. The comparison of measured to predicted values of A_d resulted in r equivalent to 0.957, a significant correlation.

The measured values of A_d as well as the calculated values of K_1 were used in conjunction with equation (9) to calculate model predictions for the upwelling radiance from the tank. Several depths for each water type were considered. Figure 5 represents both predicted and measured values of radiance reflectance (above the water surface) from clear tap water for three different water depths. The predicted values were found to correlate well with the measured values. Correlation coefficients of 0.974, 0.964, and 0.994 were calculated for the curves representing water depths of 3.81cm, 22.86cm, and 76.52cm respectively.

Comparable results were obtained for tap water with the additions of 2.7ppm and 10.8ppm rhodamine dye and are shown in figures 6 and 7 respectively. Again, predicted values were quite close to the measured values. For the tap water with 2.7ppm rhodamine dye added, values for r ranged from 0.963 to 0.983. In the case of tap water with the addition 10.8ppm rhodamine dye, values ranged from 0.959 to 0.979.

QUALITATIVE PREDICTIONS

We are now in a position to make some qualitative predictions concerning the way the reflectance of the water changes when the water is stratified. As an example, we will consider a situation which might well occur at a frontal boundary, such as at the outer edge of the Chesapeake Bay plume. The situation is illustrated in figure 8 which shows two adjacent water masses differing in color. A tongue of green water overlies a portion of the blue-green water.

Each water mass was characterized optically using measurements published in reference 6. Station 4, in Apalachee Bay where the river effluent contains significant qualitites of dissolved organic material from the large inland swamp regions, was taken as characteristic of the green water. Station 6b, in blue-green water near the mouth of the Mississippi, was chosen to represent the other water type. The irradiance reflectances and diffuse attenuation coefficients for these two stations are shown in figure 9. For this situation equation (7) becomes

$$R = R_{bg} e^{-K_g \Delta z} + R_g (1 - e^{-K_g \Delta z}) \qquad (13)$$

where R is the irradiance reflectance. The subscripts bg and g refer to blue-green (Sta. 6b) and green (Sta. 4) waters respectively. We have neglected the affects of bottom reflectance ($d \to \infty$). Since, for the purpose of modeling, the layers were assumed to be of optically infinite horizontal extent, the boundary between the two water masses is approximated in figure 8 by distinct levels.

Results are shown in figure 10 where R(0-) is plotted vs. wavelength for several thicknesses of the upper layer. When $\Delta z=0$ the reflectance is that of the blue-green water alone. As the thickness of the upper layer increases, the reflectance approaches that of optically deep green water. Note that at $\Delta=10$m, the reflectance of the two-layer system is essentially indistinguishable from that of optically deep green water. At this depth in these waters, a highly reflective bottom would be easily visible; the blue-green water has little effect due to its low reflectivity. The effective penetration depth for these waters, for the purposes of remote sensing, is only $\sim$10m although a reflective bottom might be detectable at 2 or 3 times this depth.

There are several points worth noting in comparing these curves.

(1) The change in color is quite rapid; most occur for a layer thickness of 2 attenuation lengths or less. This agrees with the conclusions of Gordon and McCluney (ref. 7).

(2) The most obvious point about figure 10 is the existence of a nodal point at 480nm. At this particular wavelength the reflectance of both water types is the same even though the optical properties may differ significantly (see figure 9). It is not possible to distinguish between the two water types by their reflectance at this nodal wave length. On the other hand, a nodal wave-length, when it exists, will provide an ideal point of reference when observing a two-component, stratified system.

(3) Less obvious, but at least as important, is the fact that the rate of change in reflectance is wavelength dependent. As can be seen from an examination of equation (13) the rate of change is entirely dependent on the spectral diffuse attenuation characteristics of the top layer which is the green water in this case.

CONCLUDING REMARKS

A relatively simple mathematical model of radiative transfer in a vertically inhomogeneous water mass has been presented. The model is quite simple in concept and is primarily designed to illustrate the ways in which water color may vary in situations which are difficult to model exactly. The preliminary experimental results presented above are

remarkably accurate, indicating that the model is faithful to reality in at least these simple situations.

Also presented were some qualitative predictions relating to a situation which might well arise in highly dynamic estuarine regions such as the Chesapeake Bay Mouth. These predictions suggest that, when the water column is stratified, considerable variation in color might occur if the top layer is variable in thickness within two attenuation lengths of the surface.

REFERENCES

1. Duntley, S. Q.; Austin, R. W.; Wilson, W. H.; Edgerton, C. F.; and Moran, S. E.: Ocean Color Analysis. Scripps Inst. of Oceanography (S.I.O.), Reference 74-10, 1974.

2. Philpot, W. D.; and Klemas, V.: Remote Detection of Ocean Waste. Ocean Optics VI, Proceedings of the Society of Photo-Optical Instrumentation Engineers, (SPIE), vol. 208, 1979, pp. 189-197.

3. Baker, K; and Smith, R. C.: Quasi-Inherent Characteristics of the Diffuse Attenuation Coefficient For Irradiance. Ocean Optics VI, Proceedings of the Society of Photo-Optical Instrumentation Engineers (SPIE), vol. 208, 1979, pp. 60-63.

4. Tyler, J.; and Smith, R. C.: Measurements of Spectral Irradiance Underwater. Gordon and Breach (New York), 1980.

5. Højerslev, N. K.: Water Color and Its Relation to Primary Production. Boundary-Layer Meteorology, vol. 18, 1980, pp. 203-220.

6. Austin, R. W.: Gulf of Mexico Ocean-Color Surface Truth Measurements. Boundary-Layer Meteorology, vol. 18, 1980, pp. 269-285.

7. Gordon, H. R.; and McCluney, W. R.: Estimation of the Depth of Sunlight Penetration in the Sea For Remote Sensing. Applied Optics, vol. 14, 1975, pp. 413-416.

Table 1

Physical Parameters of Water Tank

WATER TYPE	TRIAL	TIME	WATER DEPTH	BOTTOM TYPE
False Bottom	1	1202	0.00 cm	Flat white
Tap Water	1	1213	3.81	Flat white
	2	1232	22.86	
	3	1255	49.85	
	4	1314	76.53	
Tap Water	1	1322	74.93	Flat white
With 2.7 ppm	2	1333	50.83	
Rhodamine Dye	3	1343	25.40	
Added	4	1350	11.43	
Tap Water	1	1429	76.20	Flat white
With 10.8 ppm	2	1442	50.80	
Rhodamine Dye	3	1451	26.04	
Added	4	1458	12.70	

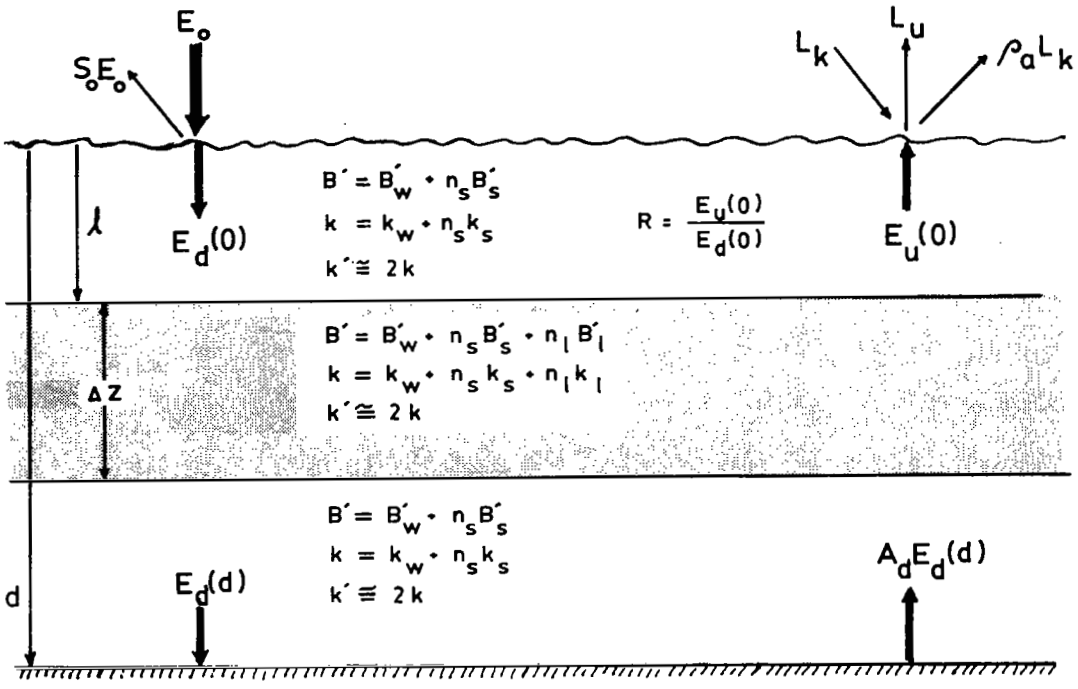

Figure 1.- Basic geometry of the multiple-layer model.

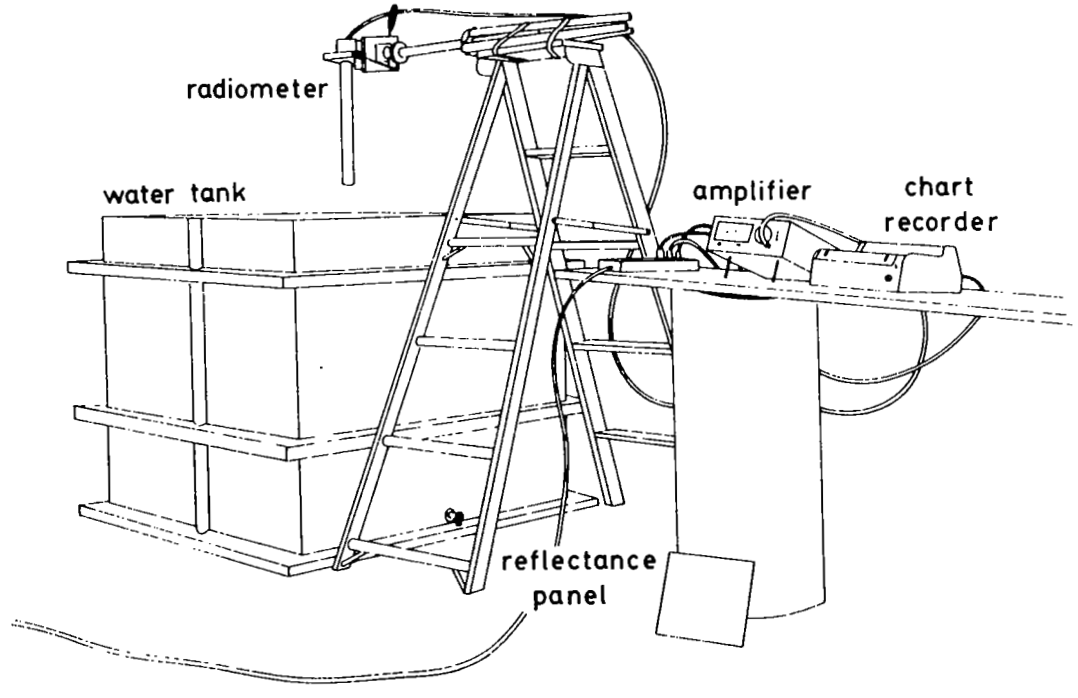

Figure 2.- Apparatus configuration to verify the multiple-layer radiance model for the case of a single homogeneously absorbing water column.

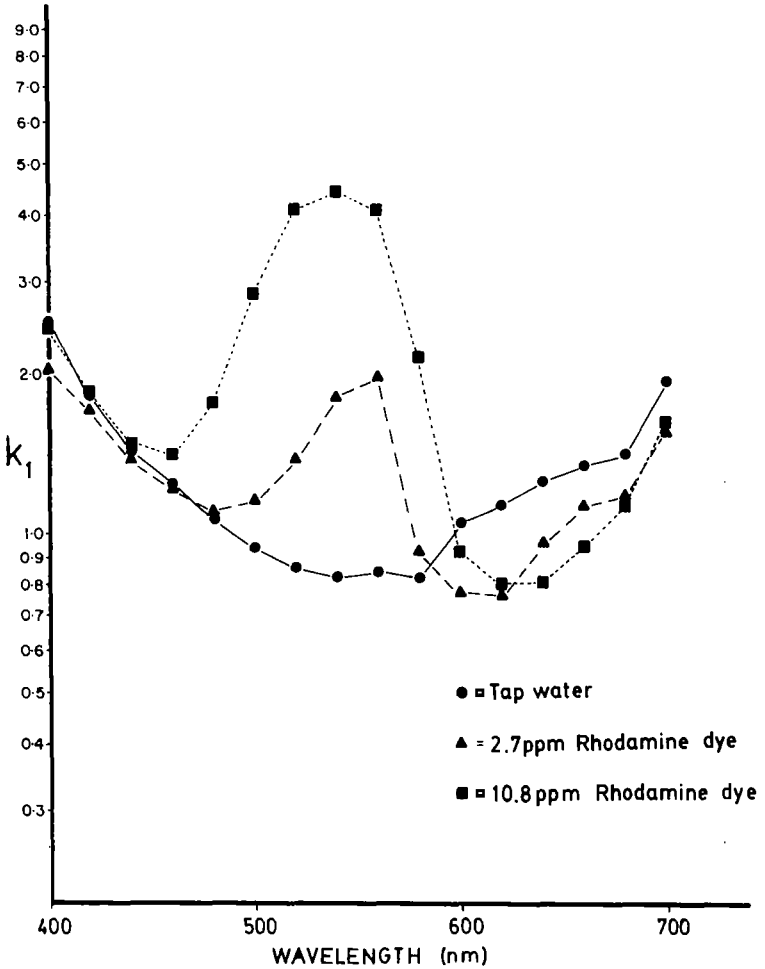

Figure 3.- Plot of the two-way attenuation coefficient versus wavelength for each water type where k_1 is equivalent to the sum of equations (1) and (2).

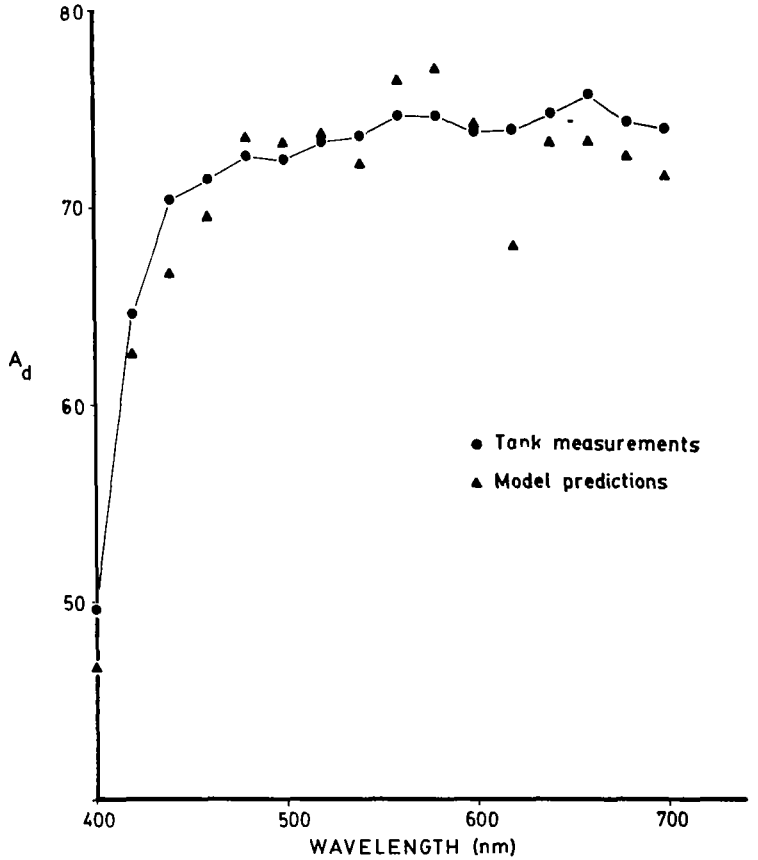

Figure 4.- Plot of direct measurements and model predictions of A_d, the reflectance of the tank bottom versus wavelength.

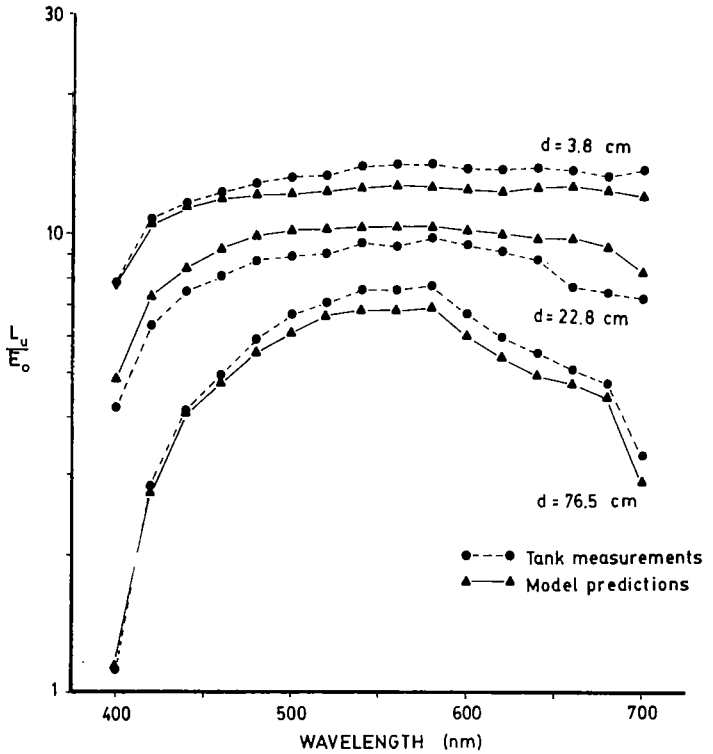

Figure 5.- Plot of measured and predicted values of volume reflectance versus wavelength for the case of clear tap water.

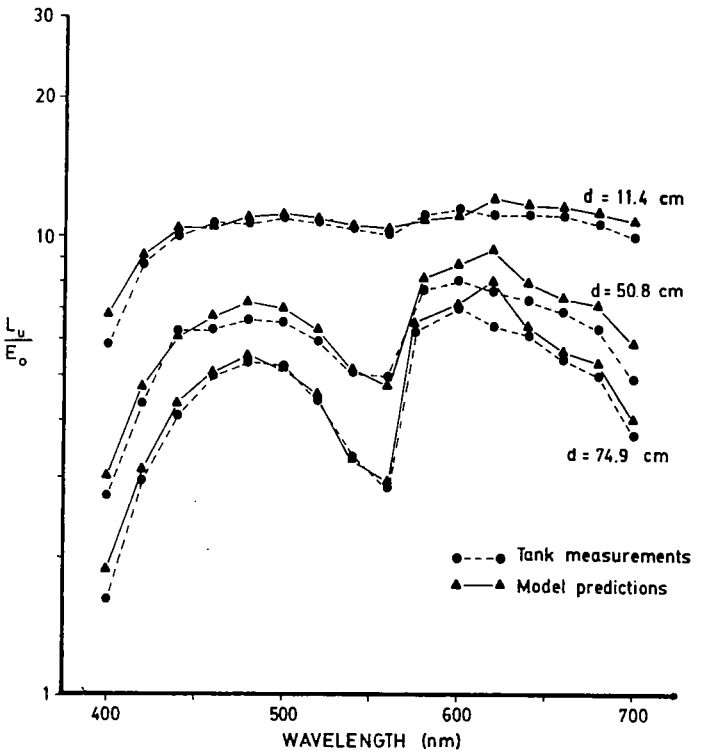

Figure 6.- Plot of measured and predicted values of volume reflectance versus wavelength for the case of clear water + 2.7 ppm Rhodamine dye.

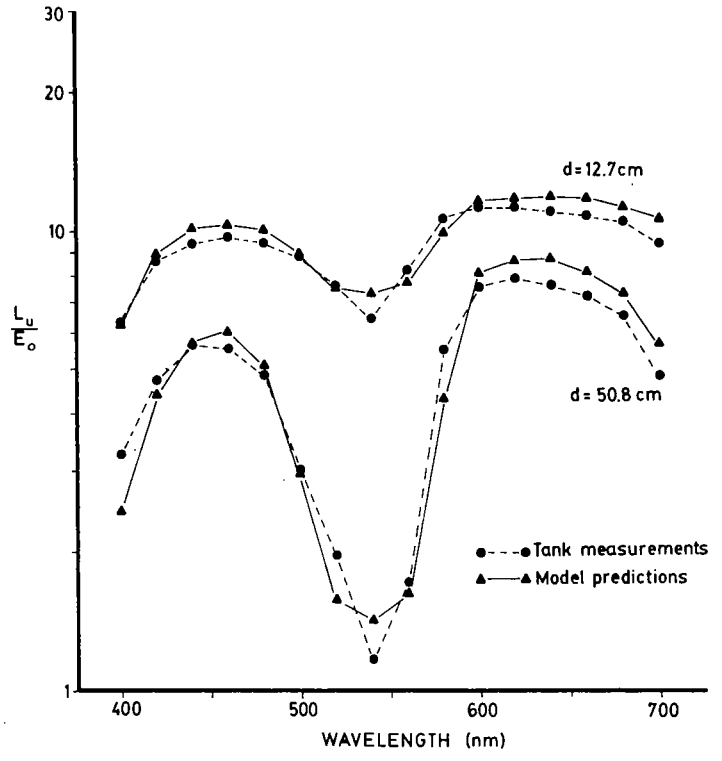

Figure 7.- Plot of measured and predicted values of volume reflectance versus wavelength for the case of clear water + 10.8 ppm Rhodamine dye.

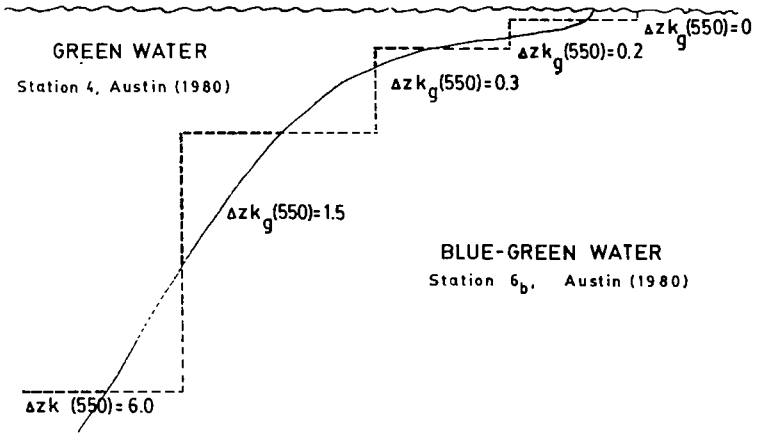

Figure 8.- Boundary between two water types. Green water overlies blue-green water. The depth is scaled to the diffuse attenuation length for the green water at 550 nm.

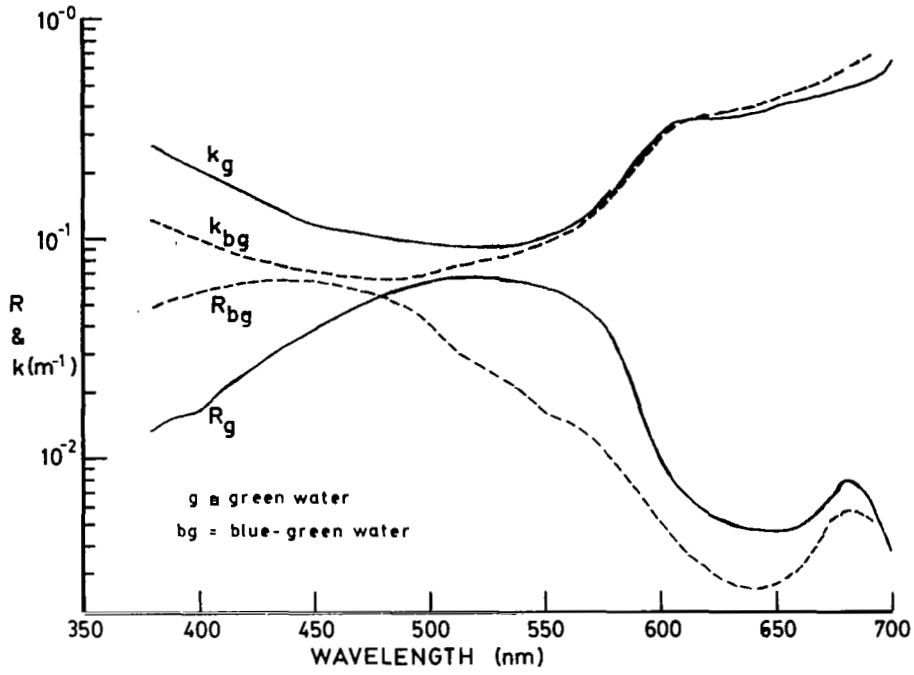

Figure 9.- Optical properties of green and blue-green waters.

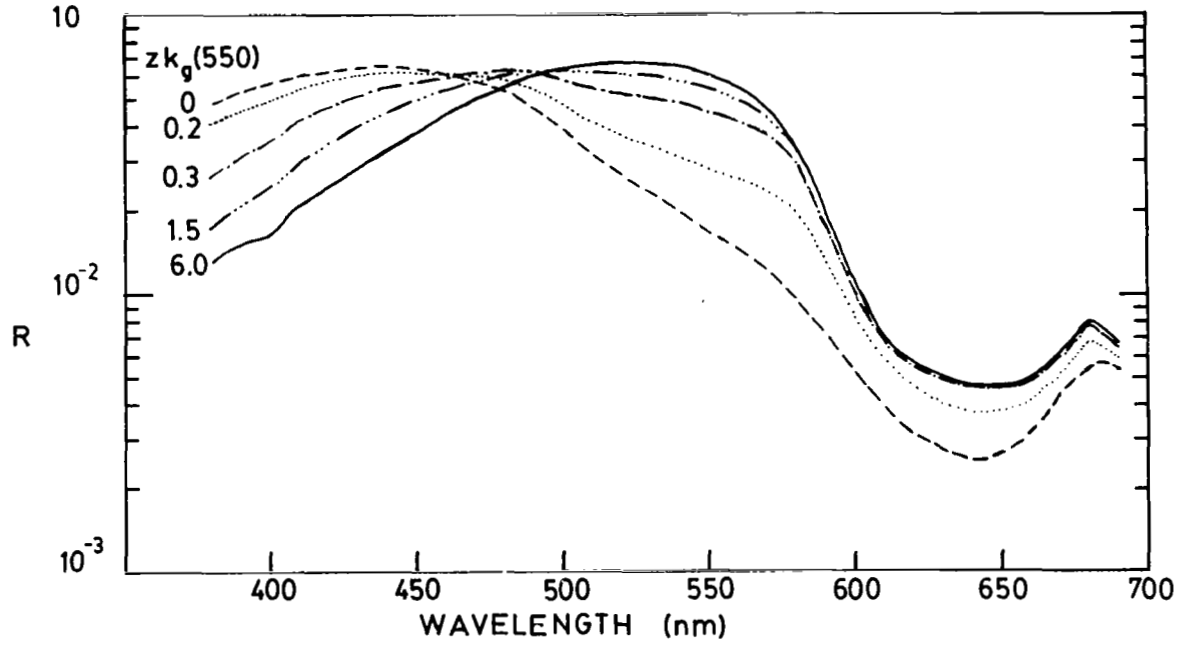

Figure 10.- Predicted irradiance reflectance for a two-layer water mass; green water overlays blue-green water.